STRUCTURE DESIGN AND THERMAL-HYDRAULIC PERFORMANCES STUDY ON TUBE-ON-SHEET HEAT EXCHANGER

Fei WANG[1,2], Guifeng GAO[3,*], Zhilong LU[1,2], Gaoyun ZHOU[1,2], Linghui Chen[4], Yongzhang CUI[5]

1. Key Laboratory of Health & Intelligent Kitchen System Integration of Zhejiang Province, Ningbo, P.R. China

2. Ningbo Fotile Kitchen Wake CO., LTD, Ningbo, P.R. China

3. College of Architecture Engineering, Shandong Yingcai University, Jinan, P.R. China

4. Zhejiang Guangtao Kitchenware CO. LTD, Ningbo, P.R. China

5. College of Thermal Energy Engineering, Shandong Jianzhu University, Jinan, P.R. China

* Guifeng GAO. Email: gaoguifeng@ycxy.com

A numerical investigation is performed to study the thermal-hydraulic performances of tube-on-sheet heat exchanger. Especially, this paper is focused on the effects of the structure parameters (fin angles, fin lengths, fin pitches, fin widths and tube arc radius) on the thermal-hydraulic characteristics of the heat exchanger. The heat exchanger optimized structural parameters are obtained. The results reveal that main structure parameters on thermal-hydraulic performance are fin angle, fin length, fin pitch and fin width. Furthermore, decreasing the fin angle, fin pitch and fin width or increasing the fin length cause thermal hydraulic performance to increase. In addition, main structure parameters on low temperature corrosion are tube arc radius and fin length. Decreasing the tube arc radius and fin length can mitigate low temperature corrosion. Furth, stainless steel is choosing as the material for the heat exchanger to reduce corrosion.

Key words: *Thermal-hydraulic performance; Numerical simulation; Elliptical tube; Corrugated fin; Stainless heat exchanger*

1. Introduction

For compact and high thermal hydraulic performance, tube-on-sheet heat exchanger is important for gas-fired on-demand water heater and boiler [1, 2]. To enhance efficiency of the heat exchanger, it is necessary to lower flue temperature and decrease air coefficient. Especially under lower flue temperature, lower air coefficient and cold water temperature, low temperature corrosion must be happened, so corrosion resistant material and new structure must be selected and designed. Common material of water heater heat exchanger are copper [3], aluminum and casting aluminum-silicon alloy [4, 5], carbon steel [3, 6], stainless steel [5, 7] and polymer heat exchanger [8].

Tubes of water heater heat exchanger always are circle tube [9, 10] or elliptic tube [2, 10, 11]. The elliptic tube structure has a better aerodynamics configuration and a lower total drag force than circle tube. Jiang et al. [12] experimentally determined that the elliptic tube heat transfer coefficient is

35-50% of the corresponding circular tube, while the drag force is only 25-30% of the circular tube. Erek et al. [1] concluded that fin pitch has a considerable influence on drag force, and increasing ellipticity of the fin tube increase the heat transfer and an important reduction in pressure drop.

Many papers have revealed the relationship between thermal hydraulic characteristics and various fin structures, such as plate fin [1, 13], strip fin [14-18], wavy fin [19], louvered fin [4,19], H-type fin, spiral fin, and slotted fin. Tao et al. [19] found that the heat exchanger with larger wavy angles, smaller fin pitch and tube row number, has better heat transfer performance and higher pressure drop. Kim et al. [4] show that the fins pitch and angle affect the thermal hydraulic performance significantly.

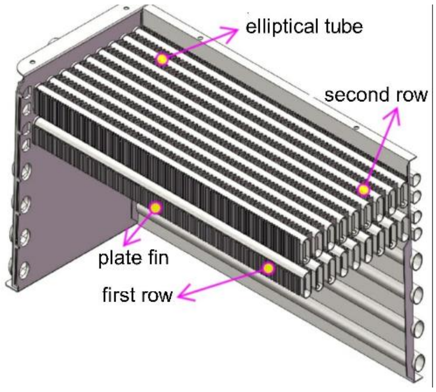

Fig.1. Stainless corrugated finned flat-elliptical tube heat exchanger

Therefore, the problems to be solved in this paper can be stated as follows. Firstly, some measures should be taken to meet the low temperature corrosion. Secondly, the structure parameters of heat exchanger should be optimizing to enhance the thermal hydraulic performance.

According above questions and studies, a new type heat exchanger is designed for gas fired water heater, showed in Fig. 1. In this work, the main purpose of 3D numerical simulation is to study effects of fin length, fin angle, fin pitch, fin width, tube arc radius, especially tube arc radius and fin width, on thermal hydraulic performance, to obtain a higher efficient and a lower corrosion heat exchanger for gas-fired water heater.

2. Model descriptions and numerical method

2.1. Physical model

Fig.2 shows a schematic diagram of one row elliptical tube and plate fin heat exchanger. Furthermore, the effects of fin structure parameters have been investigated; thermal hydraulic behavior has been predicted on gas side only. Table 1 shows the dimensions of tube and fin heat exchanger.

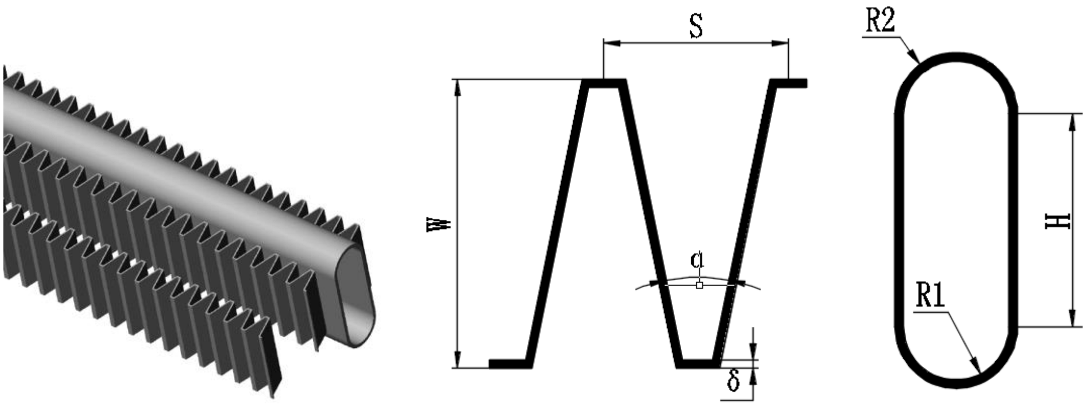

Fig.2. Structure parameters of corrugated finned flat-elliptical tube

Table 1 Main geometry data for simulated tube and fin heat exchangers

Sample No.	S(mm)	W(mm)	δ(mm)	α (°)	H(mm)	R1(mm)	R2(mm)
1	3.32	3.98	0.2	**0**	13	2.9	3.5
2	**3.32**	**3.98**	0.2	**10**	**13**	2.9	3.5
3	3.32	3.98	0.2	**20**	13	2.9	3.5
4	3.32	3.98	0.2	**30**	13	2.9	3.5
5	3.32	3.98	0.2	**40**	13	2.9	3.5
6	**4.12**	3.98	0.2	10	13	2.9	3.5
7	**4.92**	3.98	0.2	10	13	2.9	3.5
8	**5.72**	3.98	0.2	10	13	2.9	3.5
9	3.32	3.98	0.2	10	**12**	2.9	3.5
10	3.32	3.98	0.2	10	**14**	2.9	3.5
11	3.32	3.98	0.2	10	**15**	2.9	3.5
12	3.32	3.98	0.2	10	**16**	2.9	3.5
13	3.32	**4.18**	0.2	10	13	2.9	3.5
14	3.32	**4.38**	0.2	10	13	2.9	3.5
15	3.32	**4.58**	0.2	10	13	2.9	3.5
16	3.32	3.98	0.2	**10**	13	**2.4**	3.0
17	3.32	3.98	0.2	**10**	13	1.9	2.5
18	3.32	3.98	0.3	**10**	13	**1.4**	2.0

2.2. Governing equations and boundary conditions

For simplifying the mathematical model, some assumptions suggested in some articles [6,18,20], are made in the numerical simulation, as follows: (1) Viscous, steady, incompressible transition turbulent flow is presented; (2) Thermal radiation, viscosity heating and natural convection are neglected; (3) The working fluid properties is function of composition and temperature; (4) Inner wall surface are constant temperature.

The governing equations in the fluid domain are expressed as follows:

Continuity equation

$$\frac{\partial \rho}{\partial t}+\frac{\partial}{\partial x_i}(\rho u_i)=0 \tag{1}$$

Momentum equation

$$\frac{\partial}{\partial t}(\rho u_i)+\frac{\partial}{\partial x_j}(\rho u_i u_j)=-\frac{\partial p}{\partial x_i}+\frac{\partial}{\partial x_j}\left[\mu\left(\frac{\partial u_i}{\partial x_j}+\frac{\partial u_j}{\partial x_i}-\frac{2}{3}\delta_{ij}\frac{\partial u_l}{\partial x_l}\right)\right]+\frac{\partial}{\partial x_j}\left(-\rho\overline{u_i^{'}u_j^{'}}\right) \tag{2}$$

Energy equation

$$\frac{\partial}{\partial t}(\rho \mathrm{E})+\frac{\partial}{\partial x_i}\left(\rho u_i\left(\rho \mathrm{E+P}\right)\right)=\frac{\partial}{\partial x_i}\left(k_{eff}\frac{\partial T}{\partial x_i}\right) \tag{3}$$

Turbulent kinetic equation

$$\frac{\partial}{\partial t}(\rho k)+\frac{\partial}{\partial x_i}(\rho k u_i)=\frac{\partial}{\partial x_j}\left[\left(\mu+\frac{\mu_t}{\sigma_k}\right)\frac{\partial k}{\partial x_j}\right]+G_{\mathrm{k}}+G_{\mathrm{b}}-\rho\varepsilon-Y_{\mathrm{M}}+S_{\mathrm{k}} \tag{4}$$

Heat conduction equation in the solid domain

$$\frac{\partial^2 T}{\partial x^2}+\frac{\partial^2 T}{\partial y^2}+\frac{\partial^2 T}{\partial z^2}=0 \tag{5}$$

Fig.3. represents the computational domain with boundary conditions for tube-on-sheet heat exchanger. The figure also shows the coordinate system, where X is the stream wise direction, Y is the span wise direction and Z stands for the fin pitch direction. The fluid region comprises of the flow inlet, pressure outlet and the solid region includes the tube wall and fin. The outlet zone is extended with 2 times of the length of the bank to prevent the backflow while the entrance zone is extended with 150 mm to keep the uniform inlet velocity. The gas inlet is specified with the mass flow rate inlet or constant velocity-inlet boundary condition, the gas outlet with the pressure outlet boundary condition.

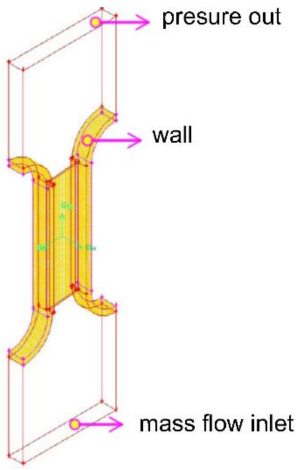

Fig.3. Computation domain

The numerical simulation is carried out using Fluent, with RNG k - ε , SIMPLE pressure-velocity coupling algorithm, and the second upwind discretization scheme for momentum, energy, turbulent kinetic energy and dissipation energy [6, 18, 20]. The convergence criterion is satisfied when the residuals of variables are less than 1×10^{-6} except for the energy where a value of 1×10^{-7} is used. Under-relaxation factors of turbulent kinetic energy, turbulent dissipation rate and turbulent viscosity are changed within the range between 0.2 and 0.4, others take the default values.

2.3. Model validation

Test section of sample No.2 is show in Fig.1, results of simulation and test are showed in Fig.4, deviation of outlet temperature and pressure drop between are within ±5%, so simulation models are valid.

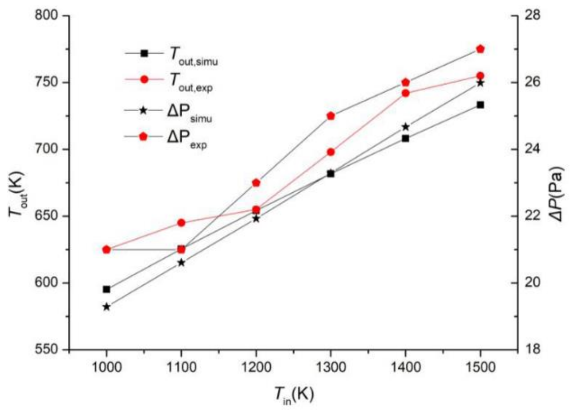

Fig.4. Temperature and pressure drop of simulation and experiment

2.4. Data reduction

To more accurately compare the thermal-hydraulic performances of tube-on-sheet heat exchanger under different structural parameters and operating conditions, some parameters are defined as follows:

The hydraulic diameter, D_h , is defined as

$$D_h = \frac{4\left[F_c H + \frac{1}{2}S(Wd + d^2 - \frac{1}{8}\pi d^2)\right]}{F_0} \tag{6}$$

Here, d is tube external diameter, d=2R2.

The Nusselt number, Nu, is defined as

$$Nu = \frac{h_o D_h}{\lambda} = \frac{Q D_h}{F_0 \Delta T_m \lambda} \tag{7}$$

Where,

$$\Delta \mathrm{T_m} = \frac{(T_{in} - T_{wall}) - (T_{out} - T_{wall})}{ln\left(\frac{T_{in} - T_{wall}}{T_{out} - T_{wall}}\right)} \tag{8}$$

$$Q = mc_p \left(T_{in} - T_{out}\right) \tag{9}$$

The friction factor, f, is calculated from the following equation

$$f = \frac{F_c}{F_0}\frac{\rho_m}{\rho_i}\left[\frac{2\Delta P \rho_i}{G_c^2} - (1 + \sigma^2) - \left(\frac{\rho_i}{\rho_0} - 1\right)\right] \tag{10}$$

Where,

$$\sigma = \frac{F_c}{F_{fr}}$$

$$F_{fr} = \frac{1}{2}(d + W)S$$

Where, ΔP is pressure drop, F_{fr} is the frontal flow area, ρ_m is the mean density, ρ_o is the outlet density, G_c is the mass flux at minimum flow area.

The Reynolds number is defined as

$$Re = \frac{\rho_i u_c D_h \frac{F_{fr}}{F_c}}{\mu} \tag{11}$$

Heat transfer and flow performance ratio θ is defined as

$$\theta = \frac{\frac{Nu}{Nu_0}}{\left(\frac{f}{f_0}\right)^{\frac{1}{3}}} \tag{12}$$

Where, Nu_0 and f_0 are based on the condition of the optimum structure, which is showed as sample No. 1in table1.

3. Result and discussion

The details of operating conditions are list in table 2. In this paper, the influence of geometrical parameters, as *α, S, H, R1* and *W*, on the thermal-hydraulic performances are studied by analyzing three factors, which are *Nu*, *f*, and *θ*.

Table 2. Details of operating conditions

Parameter	α	*S*	*H*	*R1*	*W*
Re	350-400	350-400	350-400	350-400	350-400
Mass-flow rate, m [$kgm^{-2}s^{-1}$]	0.846	0.846	0.846	0.846	0.846
Flue gas velocity[ms^{-1}]	--	3.6	--	3.6	--
Flue gas inlet temperature, $T_{flue,in}$ [K]	1000-1500	1000-1500	1000-1500	1000-1500	1000-1500
Inner wall temperature, T_w[K]	350	350	350	350	350

3.1. Tube arc radius R1

The data is divided into two groups. The fist is in the condition of constant inlet mass flow rate, in which m=0.846 $kgm^{-2}s^{-1}$. The factors are marked Nu_m, f_m, and θ_m respectively. The second is in the condition of constant inlet flue gas velocity, in which v=3.6ms^{-1}. The factors are marked Nu_v, f_v, and θ_v respectively. To illuminate the influence of tube arc radius, four circular diameters are compared. The samples from No.16 to 18 and 2 are showed in table1. With circular diameter increases, elliptical width and outer tube area enlarge, whereas fin structure does not change.

From Fig.5, it can be shown that Nu_m and f_m increase rapidly, when θ_m increases slowly with *R1* increases in the first group date. It can be concluded that the exchanger with smaller *R1* has lower pressure drop and little reduction in thermal-hydraulic performance under constant mass flow rate. In the second group date, it can be found that Nu_m and f_m increase rapidly, when θ_m decrease with *R1* increases. It suggests that the exchanger with smaller *R1* has lower pressure drop and better thermal-hydraulic performance under constant flue gas velocity.

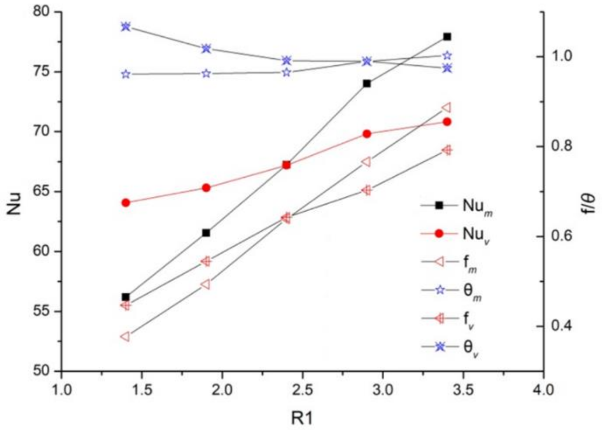

Fig.5. Thermal-hydraulic performance with arc radius under constant inlet mass flow rate and velocity

As shown in Fig.6, No.2 has larger *R1* than No.18, and the low temperature zone area at the end of the elliptical tube in No.2 is larger than No.18, when the lowest temperature of this area is lower than No.18. It demonstrates that, it will generate a low temperature zone area in the larger *R1* exchanger. The low temperature zone area could occur gas condensation and it would result in metal corrosion. To obtain better thermal-hydraulic performance, smaller area of low temperature zone and lower pressure drop, smaller *R1* should be selected. To reduce corrosion, stainless steel is choosing as the material for the heat exchanger.

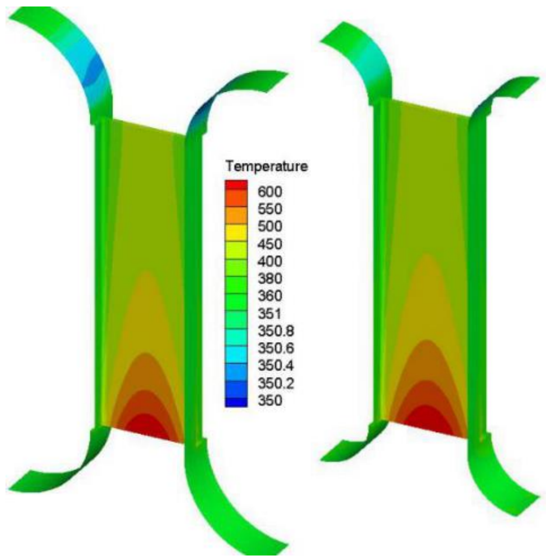

No.2 No.18

Fig.6. Temperature distribution of outer tube and fin under different arc radius

3.2. Fin width W

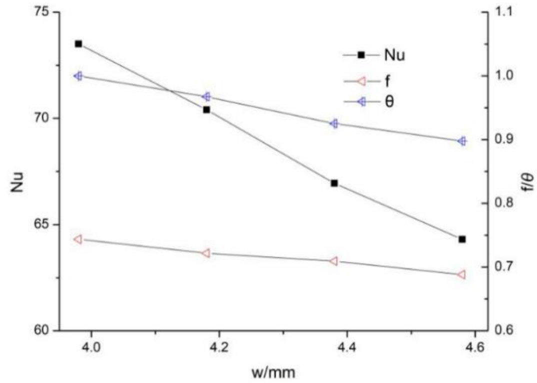

Fig.7. Thermal-hydraulic performance with different fin width under constant inlet mass flow rate

To illustrate the influence of fin width, four fin widths are compared under constant inlet mass flow rate. Samples from No.13 to 15 and 2 are showed in table1. With fin width increases, uncovered tube outer area does not change, while fin plate area increases. Fin width increases from 3.98mm to 4.58mm and total outer area increase 8.97 percent. From Fig.7, *Nu*, *f*, and *θ* decrease with the increasing fin width. Under constant inlet mass flow rate and inner temperature, inlet velocity decreases, when outlet temperature decreases slightly; heat transfer rate increases slightly, but pressure drop decreases obviously. Smaller fin width should be selected.

3.3. Fin angle α, Fin pitch S and Fin length H

Fig.8, 9, 10 have presented the variation of *Nu*, *f,* and *θ* with fin angle α, fin pitch *S* and fin length *H*. According to analyzing the curves, three conclusions are verified which had been concluded in [21]. First, with smaller α, as α= 0~20°, the heat exchanger has better thermal-hydraulic performances and lower pressure drop. Second, with smaller S and H, it has better thermal-hydraulic performance, but pressure drop becomes larger. Third, with larger *H* the low temperature of the outlet might lead to gas condensation.

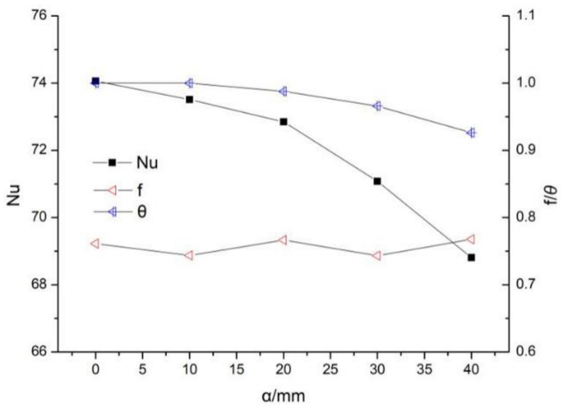

Fig.8. Thermal-hydraulic performance with different fin angles

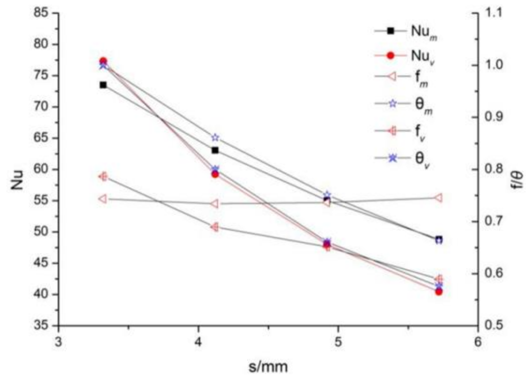

Fig.9. Thermal-hydraulic performance with different fin pitch

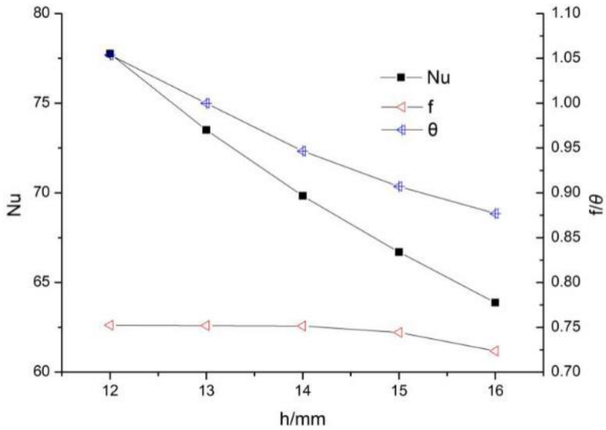

Fig.10. Thermal-hydraulic performance with different fin length

4. Conclusions

In this study, thermal-hydraulic performances of tube-on sheet heat exchanger are investigated numerically. The conclusions can be summarized as follows:

(1) Main structure parameters of tube-on sheet heat exchanger on thermal-hydraulic performances are fin angle, fin length, fin pitch and fin width. Smaller fin angle, pitch and width, higher thermal hydraulic performance. Higher fin length, higher thermal performance.

(2) Main structure parameters on low temperature corrosion are tube arc radius and fin length. Smaller arc radius and smaller fin length should be selected for reducing low temperature corrosion.

(3) To reduce corrosion, stainless steel is choosing as the material for the heat exchanger.

The numerical data for thermal-hydraulic performance are validated by test, which can be helpful to engineering applications of heat exchanger for gas-fired water heater and others.

Acknowledgement

This word is supported by Key research and development program of Shandong Province (NO.2018GSF117015), and Shandong Jianzhu University doctor Foundation (NO.XNBS1217).

Nomenclature

d	tube external diameter (mm)	$T_{ave,flueout}$	average temperature of outlet flue gas (K)
D_h	hydraulic diameter (m)	$T_{ave,fin}$	average temperature of fin (K)
f	friction factor	T_{fluein}	inlet temperature of flue gas (K)
f_0	f based on tube without any fin	$T_{flueout}$	outlet temperature of flue gas (K)
F_0	total outside superficial area (m^2)	T_{wall}	inner wall temperature of tube (K)
F_c	minimum flow area (m^2)	ΔT_m	log-mean temperature difference (K)
F_{fr}	inlet frontal flow area (m^2)	u_c	velocity at the minimum cross sectional area (m/s)
F_{fin}	fin effective heat transfer area (m^2)	W	fin width (mm)
$F_{G\text{-}fin}$	fin geometric superficial area (m^2)	Greek symbols	
$F_{G\text{-}tube}$	tube geometric superficial area (m^2)	α	fin angle (°)
F_{tube}	tube effective heat transfer area (m^2)	α_ε	inverse effective Prandtl numbers for ε
G_c	mass flux at minimum flow area (kgm^{-2}.s^{-1})	α_k	inverse effective Prandtl numbers for k
H	fin length (mm)	δ	fin thickness (mm)
Nu	Nusselt number	ρ	density (kgm^{-3})
Nu_0	Nu based on tube without any fin	ρ_m	mean density (kgm^{-3})
ΔP	pressure drop (Pa)	ρ_i	inlet density (kgm^{-3})
Q	total heat transfer rate (W)	ρ_o	outlet density (kgm^{-3})
Q_{fin}	fin heat transfer rate (W)	η	heat transfer and flow performance ratio
Q_{tube}	tubes heat transfer rate (W)	η_{fin}	fin efficiency
$R1$	tube inner arc radius	θ	fin coefficient
$R2$	tube outer arc radius	λ	thermal conductivity (Wm^{-1}.K^{-1})
Re	Reynolds number	μ	dynamic viscosity (kgm^{-1}.s^{-1})
S	fin pitch (mm)		

Reference

[1] Ereka, A., *et al.*, Effect of geometrical parameters on heat transfer and pressure drop characteristics of plate fin and tube heat exchangers. *Applied Thermal Engineering*.25 (2005), pp. 2421-2431

[2] Antonescua, N., *et al.*, Computational model for a condensing boiler with finned tubes heat Exchanger. *Energy Procedia,* 112 (2017), pp. 555-562

[3] González, A. M., *et al.*, A hybrid numerical-experimental analysis of heat transfer by forced convection in plate-finned heat exchangers. *Applied Thermal Engineering*.148 (2019), pp. 363-370

[4] Kim, M., *et al.*, Air-side performance of brazed aluminum heat exchangers under dehumidifying conditions. *International Journal of refrigeration,* 25(2002), pp. 924-934

[5] Lee, S., *et al.*, Performances of a heat exchanger and pilot boiler for the development of a condensing gas boiler. *Energy*, 36 (2011), pp. 3945-3951

[6] Xu, J., *et al*., Numerical simulation of the flow and heat-transfer characteristics of an aligned external three-dimensional rectangular-finned tube bank. *Applied Thermal Engineering*.145 (2018) 10-122.

[7] Kundu, B., *et al*., Performance Analysis of Plate Fins Circumscribing Elliptic Tubes. *Heat transfer engineering*. 27(2006), 3, pp.86-94.

[8] Trojanowski, R., *et al*., Polymer heat exchanger design for condensing boiler applications. *Applied Thermal Engineering*, 103(2016), 150-158

[9] Zhang, G. H., *et al*., Review of experimentation and modeling of heat and mass transfer performance of fin-and-tube heat exchangers with dehumidification. *Applied Thermal Engineering*, 146 (2019) 701-717.

[10] Deepakkumar, R., *et al*., Air side performance of finned-tube heat exchanger with combination of circular and elliptical tubes. *Applied Thermal Engineering*.119 (2017)360-372.

[11] Wang, Q., *et al*., Analysis on thermal hydraulic performance of the elliptical tube in the finned-tube heat exchanger by new method. *International Journal of Heat and Mass Transfer*.134 (2019), pp. 388-307.

[12] Jang, J., *et al*., Experimental and 3-D Numerical Analysis of the Thermal-Hydraulic Characteristics of Elliptic Finned-Tube Heat Exchangers. *Heat transfer engineering*. 19(1998), 4, pp.55-67.

[13] Li, M., *et al*., 3D numerical simulation of heat and mass transfer of fin-and-tube heat exchanger under dehumidifying conditions. *International Journal of Heat and Mass Transfer*.127(2018), pp. 597-610.

[14] Liu, Z. Y., *et al*., Numerical study of the air inlet angle influence on the airside performance of plate-fin heat exchangers. *Applied Thermal Engineering*. 89 (2015), pp. 356-364.

[15] Doohan, R. S., *et al*., Exergy based optimization and experimental evaluation of plate fin heat exchanger. *Applied Thermal Engineering*.102 (2016), pp. 80-90.

[16] Guo, K., *et al*., Design optimisation of multi-stream plate fin heat exchangers with multiple fin types. *Applied Thermal Engineering*.131 (2018), pp. 30-40.

[17] Yang, H. Z., *et al*., Effect of fin types and Prandtl number on performance of plate-fin heat exchanger: Experimental and numerical assessment. *Applied Thermal Engineering*.144 (2018), pp. 726-735.

[18] Ahmed, H., *et al*., Optimization of thermal design of ribbed flat-plate fin heat sink. *Applied Thermal Engineering*.102 (2016), pp. 1422-1432.

[19] Tao, Y. B., *et al*., Three-dimensional numerical study of wavy fin-and-tube heat exchangers and field synergy principle analysis. *International Journal of Heat and Mass Transfer,* 50 (2007), pp. 1163-1175.

[20] Cui, Y. Z., *et al*., Three-dimension numerical simulation of thermal hydraulic performance of a circular tube with edgefold twisted tape inserts. *Journal of Hydrodynamics,* 22(2010), 5, 662-670.

[21] Gao, G., et al., Structural Parameters Study on Stainless-Steel flat-tube heat exchangers with corrugated fins. *Thermal Science,* 24(2020), 5A, 2743-2756.